ANALYTICAL INVESTIGATION OF PERIODIC COPLANAR WAVEGUIDES

Teng-Kai Chen[1, 2, *] and Gregory H. Huff[1]

[1]Department of Electrical and Computer Engineering, Texas A & M University, College Station, TX 77843, USA

[2]Fujitsu Laboratories of America, Inc., Sunnyvale, CA 94085, USA

Abstract—This paper presents an analytical formula to evaluate even- and odd-mode characteristics of infinitely parallel coplanar waveguides (CPW) with the same dimensions in each CPW, given name as periodic coplanar waveguides (PCPW). The analysis yields a closed-form expression based on the quasi-TEM assumption and conformal mapping transformation. Calculated results show that both the even- and odd-mode characteristic impedances are in good agreements with the results generated by numerical solvers and available experimental data. The results are important especially for highly demand on miniaturization of circuit design to place multiple CPWs in parallel.

1. INTRODUCTION

Coplanar waveguides (CPW) have been widely used in the design of microwave integrated circuits and printed circuit board because the signal conductor and ground planes are on the same surface of dielectric layer and they are useful for the transistor-based circuits. The ideal CPW consists of infinitely thick dielectric substrate with two semi-infinite ground conductors on both sides. The first analytic formula for this ideal configuration is given by Wen [1] using conformal mapping. In actual implementation, the CPW structures are neither of infinite substrate nor infinite lateral extent and the computation of their propagation characteristics has received great attention with a variety of analytical and numerical techniques [2–5]. However, the demands on designing high-speed circuits and systems with the increase of integration density have led to multiconductor interconnects [6]. Many

systems currently use signaling interfaces in which large numbers
of CPW are routed in parallel. In order to maximize the circuit
density, the ground conductor width should be as small as possible, but
truncating lateral ground planes and placing CPW close to each other
also increase line-to-line coupling. To optimize the electrical properties
of multi-CPW interconnects, the analysis must be investigated.

The extraction of capacitances per unit length (p.u.l.) of
multiconductor quasi-TEM transmission lines is known as an
important parameter on the transmission characteristics. Many
numerical extraction methods for multiconductor system include finite
difference methods (FDM) [7, 8] and spectral domain method [9–11].
Although they are accurate and adaptable to many configurations,
the quasi-TEM analysis requiring less computational effort can yield
useful results in the design phase, but very few analytical methods were
found on the multiconductor coplanar system. An exact analysis for
the three coupled strip lines in a homogeneous dielectric material was
studied in [12] through conformal mapping techniques. More coupled
striplines shielded in a metal box were studied in [13]. For the open-
space transmission lines, the coupled CPW (two coplanar conductors
with infinite lateral ground on both sides) and the parallel CPW (two
coplanar conductors separated by a coplanar finite ground in-between
with infinite lateral ground) were discussed in [14–16], respectively.
More coplanar conductors placed closely with lateral ground strips are
discussed in [13, 17] for high-speed interconnections. The guarding
ground can also be inserted between the signal conductors to improve
the high-speed performance further [18, 19], which is then similar to
the CPW structure for individual transmission line. To the author's
best knowledge, the analytical treatment of parallel multi-CPWs
(multiconductors separated by multiple coplanar finite grounds, as
shown in Figure 1) has not been explicitly given yet.

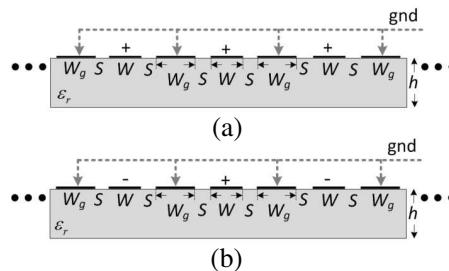This paper analyzes a circumstance in which several CPW

Figure 1. Configuration of periodic coplanar waveguides (PCPW) in
(a) even (common) mode and (b) odd (differential) mode.

transmission lines are parallel. The analysis of wave propagation, characteristic impedance, and coupling effect of an individual line in a multiple transmission line environment is a common treatment (as an equivalent single transmission line) during the initial design of a full system, and followed here. For simplification and to investigate the properties of several parallel CPWs, a configuration called periodic coplanar waveguide (PCPW) with identical dimension in each periodic cell is a suitable model to analyze, as shown in Figure 1. It should be noted that this work is different from the periodic CPW structures in [20], which could be described as periodic loaded CPWs since the wave propagation properties are modified by periodically placed elements.

The paper is structured as follows. After a short review of conformal mapping approach for the evaluation of PCPW characteristics, the closed-form expressions of characteristic impedance and effective dielectric constant are presented. Finally, the results calculated by the proposed expressions are in excellent agreement with those obtained by full-wave simulation and experimental data.

2. CONFORMAL MAPPING ANALYSIS

Figure 1 shows the configuration of PCPW, consisting of a conductor strip of width W on top of dielectric substrate of ε_r and thickness h with two lateral ground conductors of width W_g on both sides of a spacing S. Due to the periodicity in the PCPW, the unit cell as shown in Figure 2(a) is taken for the analysis, where the boundary plane between two adjacent cells can be modeled as perfect magnetic conductor (PMC) walls or perfect electric conductor (PEC) walls for even-or odd-mode propagation, respectively. The assumption for quasi-static conformal mapping analysis requires the dimensions of PCPW $L_p = 2S + W + W_g \ll \lambda_g/2$ (λ_g is guided wavelength), which is usually valid for the application of PCB, packaging, or RF/microwave circuit design. A PMC wall can then be placed at the middle plane of the signal strip with an assumption of symmetric field distribution. For the sake of clarity, PCPW on a single-layered substrate is sufficient to explain conformal mapping steps, while the derivation presented below is also applicable to the general case of multilayered structures with/without conductor-backed plate.

The characteristic impedance Z_0 and effective dielectric constant ε_{reff} that propagating wave sees can be completely determined from the total p.u.l. capacitance C
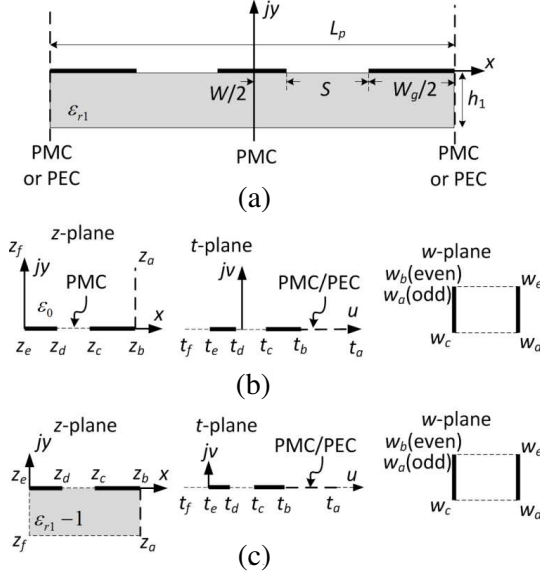
$$C = C_0 + C_1, \qquad (1)$$

Figure 2. (a) Unit cell of PCPW, (b) conformal mapping steps for C_0, and (c) conformal mapping steps for C_1.

where C_0 and C_1 represent the capacitance when the partial field distribution reside in free space and inside the dielectric material of $(\varepsilon_{r1}-1)$, respectively [21]. The partial capacitance technique [3, 22, 23] is applied to evaluate these p.u.l. capacitance of PCPW, which models the air/dielectric and dielectric/dielectric interfaces as PMC. In the following analysis, the metal strips have negligible thickness with perfect conductivity and the dielectric layers are lossless.

2.1. Common Mode

The symmetry of the PCPW structure allows analysis performed on one of quadrants in the z-plane and then uses equivalent circuit principle to evaluate the even mode p.u.l. capacitance C_{e0} and C_{e1}. Figure 2(b) shows the conformal mapping steps for the calculation of C_{e0}. The z-plane for this topology has the coordinates $z_b = L_p/2$, $z_c = S + W/2$, $z_d = W/2$, and $z_e = 0$. The transformation

$$t = -\cos\left(\frac{2\pi z}{L_p}\right) \tag{2}$$

maps the z-plane onto the upper half t-plane and then transformation

$$w = \int^t \frac{dt'}{\sqrt{(t'^2 - 1)(t' - t_c)(t' - t_d)}} \tag{3}$$

maps the upper half t-plane onto a rectangle in the w-plane. After transformation, the p.u.l. capacitance C_{e0} of air-filled PCPW can be directly obtained by

$$C_{e0} = 4\varepsilon_0 \frac{K(k_{e0})}{K(k'_{e0})}, \tag{4}$$

where $K(k_{e0})$ and $K(k'_{e0})$ are the complete elliptic integral of first kind with the modulus k_{e0} and the complementary modulus k'_{e0} expressed by

$$k_{e0} = \cot\left(\frac{\pi}{2}\frac{2S + W}{L_p}\right)\tan\left(\frac{\pi}{2}\frac{W}{L_p}\right) \tag{5}$$

$$k'_{e0} = \sqrt{1 - k_{e0}^2} \tag{6}$$

Figure 2(c) shows the conformal mapping steps for evaluation of C_{e1}. The transformation

$$t = \text{sn}^2\left(K_1\frac{2z}{L_p}, r_1\right) \tag{7}$$

maps the z-plane of PCPW bounded inside the dielectric material onto the upper-half t-plane, where $\text{sn}(u, r_1)$ is the Jacobian elliptic function with a variable u and a modulus r_1 determined by

$$q_1 = \exp\left(-\pi\frac{2h_1}{L_p}\right) \tag{8}$$

$$r_1 = 4\sqrt{q_1}\prod_{n=1}^{\infty}\left(\frac{1 + q_1^{2n}}{1 + q_1^{2n-1}}\right)^4, \tag{9}$$

and $K_1 = K(r_1)$ is evaluated by

$$K_1 = \frac{\pi}{2} + 2\pi\sum_{s=1}^{\infty}\frac{q_1^s}{1 + q_1^{2s}}. \tag{10}$$

Then the transformation

$$w = \int^t \frac{dt'}{\sqrt{t'(t' - 1)(t' - t_c)(t' - t_d)}} \tag{11}$$

maps the upper-half t-plane onto a rectangle in the w-plane. The p.u.l. capacitance C_{e1} is obtained by

$$C_{e1} = 2\varepsilon_0(\varepsilon_{r1} - 1)\frac{K(k_{e1})}{K(k'_{e1})}, \tag{12}$$

where the modulus k_{e1} and the complementary modulus k'_{e1} is given by

$$k_{e1} = \frac{\mathrm{sn}\left(K_1 \frac{W}{L_p}, r_1\right)}{\mathrm{sn}\left(K_1 \frac{2S+W}{L_p}, r_1\right)} \sqrt{\frac{1 - \mathrm{sn}^2\left(K_1 \frac{2S+W}{L_p}, r_1\right)}{1 - \mathrm{sn}^2\left(K_1 \frac{W}{L_p}, r_1\right)}} \tag{13}$$

$$k'_{e1} = \sqrt{1 - k_{e1}^2}. \tag{14}$$

The total p.u.l. capacitance C_e is the sum of all partial capacitances and is expressed by

$$C_e = 4\varepsilon_0 \varepsilon_{reff}^{\mathrm{even}} \frac{K\left(k_{e0}\right)}{K\left(k'_{e0}\right)}, \tag{15}$$

where the effective dielectric constant is given in

$$\varepsilon_{reff}^{\mathrm{even}} = 1 + \frac{1}{2}\left(\varepsilon_{r1} - 1\right) \frac{K\left(k_{e1}\right)}{K\left(k'_{e1}\right)} \frac{K\left(k'_{e0}\right)}{K\left(k_{e0}\right)}. \tag{16}$$

The common-mode characteristic impedance is then given by

$$Z_0^{\mathrm{even}} = \frac{30\pi}{\sqrt{\varepsilon_{reff}^{\mathrm{even}}}} \frac{K\left(k'_{e0}\right)}{K\left(k_{e0}\right)} \tag{17}$$

2.2. Differential Mode

For the odd mode propagation, the boundary of unit cell is assumed PEC. The transformation (2) maps the z-plane onto the upper half t-plane, and then transformation

$$w = \int^t \frac{dt'}{\sqrt{(t'+1)\left(t'-t_c\right)\left(t'-t_d\right)}} \tag{18}$$

maps the upper half t-plane onto a rectangle in the w-plane. After transformation, the odd mode p.u.l. capacitance C_{o0} of air-filled PCPW can be obtained by

$$C_{o0} = 4\varepsilon_0 \frac{K\left(k_{o0}\right)}{K\left(k'_{o0}\right)} \tag{19}$$

$$k_{o0} = \sin\left(\frac{\pi}{2}\frac{W}{L_p}\right) \bigg/ \sin\left(\frac{\pi}{2}\frac{2S+W}{L_p}\right) \tag{20}$$

$$k'_{o0} = \sqrt{1 - k_{o0}^2}. \tag{21}$$

Figure 2(c) also shows the conformal mapping steps for evaluation of C_{o1}. The transformation of (7)–(10) maps z-plane to t-plane and then the transformation

$$w = \int^t \frac{dt'}{\sqrt{t'\left(t' - t_a\right)\left(t' - t_c\right)\left(t' - t_d\right)}} \tag{22}$$

maps the upper half t-plane onto a rectangle in the w-plane. The p.u.l. capacitance C_{o1} is obtained by

$$C_{o1} = 2\varepsilon_0 \left(\varepsilon_{r1} - 1\right) \frac{K\left(k_{o1}\right)}{K\left(k'_{o1}\right)} \tag{23}$$

$$k_{o1} = \frac{\operatorname{sn}\left(K_1 \frac{W}{L_p}, r_1\right)}{\operatorname{sn}\left(K_1 \frac{2S+W}{L_p}, r_1\right)} \sqrt{\frac{1 - r_1^2 \operatorname{sn}^2\left(K_1 \frac{2S+W}{L_p}, r_1\right)}{1 - r_1^2 \operatorname{sn}^2\left(K_1 \frac{W}{L_p}, r_1\right)}} \tag{24}$$

$$k'_{o1} = \sqrt{1 - k_{o1}^2} \tag{25}$$

The total p.u.l. capacitance C_o for odd mode propagation is expressed in

$$C_o = 4\varepsilon_0 \varepsilon_{reff}^{\text{odd}} \frac{K\left(k_{o0}\right)}{K\left(k'_{o0}\right)}, \tag{26}$$

where the effective dielectric constant is given in

$$\varepsilon_{reff}^{\text{odd}} = 1 + \frac{1}{2}\left(\varepsilon_{r1} - 1\right) \frac{K\left(k_{o1}\right)}{K\left(k'_{o1}\right)} \frac{K\left(k'_{o0}\right)}{K\left(k_{o0}\right)}. \tag{27}$$

The odd-mode characteristic impedance is then given by

$$Z_0^{\text{odd}} = \frac{30\pi}{\sqrt{\varepsilon_{reff}^{\text{odd}}}} \frac{K\left(k'_{o0}\right)}{K\left(k_{o0}\right)} \tag{28}$$

2.3. Multilayer Extension

Figure 3 shows a PCPW structure embedded in a set of infinite number of dielectric layers. The parallel partial capacitance approximation can be easily extended to multilayer cases as demonstrated in [22]. The limitation of partial capacitance technique is discussed in [24], which states that the parallel partial capacitance (PPC) approach is valid only when the dielectric constant is decreasing layer by layer away from the PCPW structure. When the dielectric constant is increasing away from the PCPW structure, the series partial capacitance (SPC) approach can be used to evaluate the quasi-TEM properties. Despite this limitation, the analysis in this section is still applicable to most
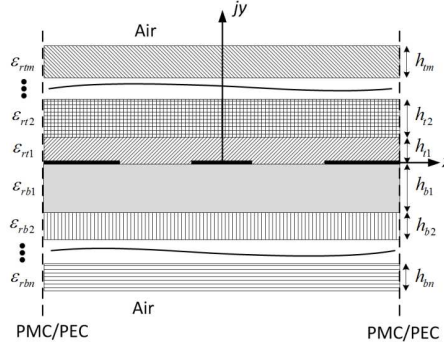
Figure 3. PCPW in multilayered dielectric structure.

applications. For the even mode, the effective dielectric constant is redefined as

$$
\varepsilon_{reff}^{\text{even}} = 1 + \sum_i \xi_{ei}\varepsilon^{(i)}, \quad i = \begin{cases} t1, \ldots, tm; & \text{for top layers} \\ b1, \ldots, bn; & \text{for bottom layers} \end{cases} \tag{29}
$$

$$
\xi_{ei} = \frac{1}{2} \frac{K\left(k_{ei}\right)}{K\left(k_{ei}'\right)} \frac{K\left(k_{e0}'\right)}{K\left(k_{e0}\right)} \tag{30}
$$

$$
k_{ei} = \frac{\text{sn}\left(K_i \frac{W}{L_p}, r_i\right)}{\text{sn}\left(K_i \frac{2S+W}{L_p}, r_i\right)} \sqrt{\frac{1 - \text{sn}^2\left(K_i \frac{2S+W}{L_p}, r_i\right)}{1 - \text{sn}^2\left(K_i \frac{W}{L_p}, r_i\right)}} \tag{31}
$$

$$
r_i = 4\sqrt{q_i} \prod_{n=1}^{\infty} \left(\frac{1 + q_i^{2n}}{1 + q_i^{2n-1}}\right)^4, \quad q_i = \exp\left(-\pi \frac{2h^{(i)}}{L_p}\right) \tag{32}
$$

$$
\varepsilon^{(i)} = \varepsilon_{ri} - \varepsilon_{r(i+1)}, \quad \text{with} \begin{cases} \varepsilon_{rt(m+1)} = 1 \\ \varepsilon_{rb(n+1)} = 1 \end{cases} \tag{33}
$$

$$
h^{(i)} = \begin{cases} \displaystyle\sum_{i=t1}^{tm} h_i, & \text{for top layers} \\ \displaystyle\sum_{i=b1}^{bn} h_i, & \text{for bottom layers} \end{cases} \tag{34}
$$

For the odd mode, the effective dielectric constant is redefined as

$$
\varepsilon_{reff}^{\text{odd}} = 1 + \sum_i \xi_{oi}\varepsilon^{(i)}, \quad i = \begin{cases} t1, \ldots, tm; & \text{for top layers} \\ b1, \ldots, bn; & \text{for bottom layers} \end{cases} \tag{35}
$$

$$\xi_{oi} = \frac{1}{2} \frac{K\left(k_{oi}\right)}{K\left(k'_{oi}\right)} \frac{K\left(k'_{o0}\right)}{K\left(k_{o0}\right)} \tag{36}$$

$$k_{oi} = \frac{\text{sn}\left(K_i \frac{W}{L_p}, r_i\right)}{\text{sn}\left(K_i \frac{2S+W}{L_p}, r_i\right)} \sqrt{\frac{1 - r_i^2 \text{sn}^2\left(K_i \frac{2S+W}{L_p}, r_i\right)}{1 - r_i^2 \text{sn}^2\left(K_i \frac{W}{L_p}, r_i\right)}}, \tag{37}$$

where the geometric parameters are defined in (32)–(34).

3. VALIDATION AND DISCUSSIONS

This section will present the calculated results by conformal mapping analysis to verify the derived expressions as well as to investigate the properties of PCPW. Comprehensive comparisons with the results of full-wave analysis and available experimental data in literatures will be presented in this section and demonstrate that the derived formulas are accurate for most of the application range of physical dimensions and available dielectric materials. Note that all functions used in the analysis (e.g., elliptic integrals of first kind) are available in most mathematical software packages. However, as the modulus k is close to 1 or 0, the calculation of Jacobian elliptic function $\text{sn}(u, k)$ will be saturated due to double-precision error. For $2h_1/L_p < 0.1$ ($k \to 1$), the function can be simplified by

$$\text{sn}\left(u, k\right) = \tanh u \tag{38}$$

For $2h_1/L_p > 100$ ($k \to 0$), the approximation is given by

$$\text{sn}\left(u, k\right) = \sin u \tag{39}$$

3.1. PCPW with Infinite Periodicity

Figure 4 shows the characteristic impedance of single layered PCPW operating in even mode. The parameters used in this computation are $\varepsilon_{rb1} = 13$, $h_{b1} = 1.5\,\text{mm}$, and $W + 2S = 3\,\text{mm}$. As expected, the agreement is excellent between the calculated results with $W_g = 10(W + 2S)$ and those from [25] using full wave analysis with assumption of infinite lateral ground. It is intuitive to see that the curves are dependent on the lateral ground width W_g. In this case, the PCPW with $W_g > 2(W + 2S)$ can be considered as an isolated CPW with infinite lateral grounds, where we can denote $(W + 2S)$ as the dimension of isolated CPW. As each CPW is placed closer than the dimension of isolated CPW in periodic structure, e.g., $W_g < (W + 2S)$, the coupling between transmission lines results in impedance change.

Figure 5 shows the characteristic impedance of PCPW on two-layered substrate, where the calculations are carried out with the
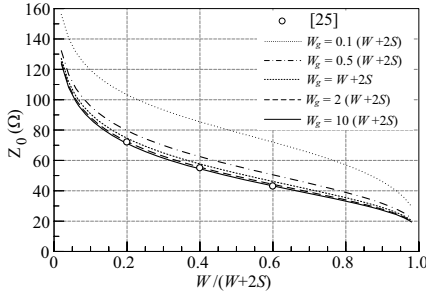
Figure 4. Characteristic impedance of single layered PCPW with $\varepsilon_{rb1} = 13$, $h_{b1} = 1.5\,\text{mm}$, and $W + 2S = 3\,\text{mm}$.
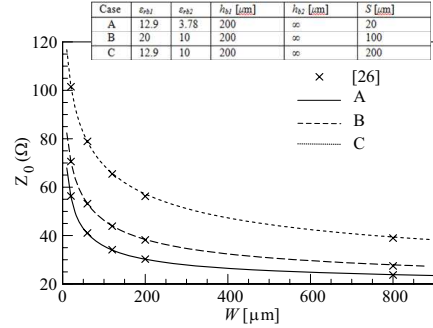
Figure 5. Characteristic impedance of two-layered PCPW with infinite periodicity.

parameters listed in Figure 5 and large lateral ground width of $W_g = 10(W + 2S)$. The calculated results are compared with the numerical results taken from [26] using spectrum domain method. It shows an excellent agreement on multilayered isolated CPW structures.

3.2. PCPW with Equal Strip Width

In this section, the PCPWs with fixed periodicity of $W + S = 2.5\,\text{mm}$ and equal strip width of $W_g = W$ are analysed. The field distribution now has dependence on both substrate height h and the metallization ratio χ defined by

$$\chi = \frac{W}{W + S} \tag{40}$$

Specifically, for a fixed metallization ratio χ, smaller values of $(W + S)/h$ correspond to smaller conductor spacing S compared to h and an increased field distribution within the substrate; this increases the total p.u.l. capacitance and decreases the characteristic impedance of the propagating modes. The characteristic impedance in even- and odd-modes are calculated and compared with the simulated data from COMSOL Multiphysics [27], a proven commercial solver based on finite element method. The corresponding PCPW CAD model consists of nine unit cells of CPW. A range of commercially available substrate of various heights and dielectric constants are used to validate the proposed analytical formulas. The simulated characteristic impedance are obtained by p.u.l. capacitance C and C_0 extracted from the center cell with/without dielectric material present, respectively.
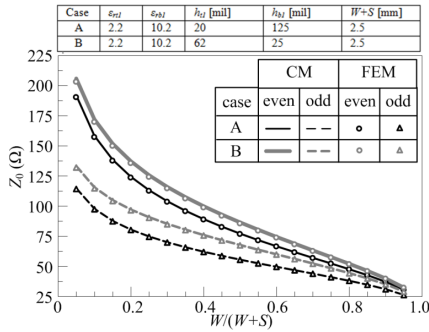
Figure 6. Even- and odd-mode characteristic impedance of PCPW embedded in dielectric materials versus metallization ratio obtained by conformal mapping (CM) and finite element method (FEM).
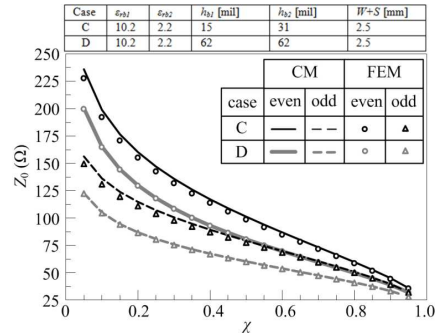
Figure 7. Even- and odd-mode characteristic impedance of PCPW residing on two-layer substrate of finite thickness obtained by conformal mapping (CM) and finite element method (FEM).

Figures 6 and 7 show the even- and odd-mode impedance of PCPW embedded in two dielectric materials of different heights and on top of two-layered substrate, respectively, with parameters listed in the figures. Overall, the conformal mapping results agree with the numerical simulations within an error of 3.5%, which is also acceptable for a numerical error. Both even- and odd-mode impedance and the difference between them increase as the metallization ratio decreases. In the Case C of Figure 7, the discrepancy is observed in the thin substrate due to the approximation of modeling dielectric/air interface as a PMC, while for higher metallization ratio, the higher field concentration inside the dielectric materials results in a more accurate PMC model on interface. In general, the discrepancy in odd-mode is larger than that in even-mode because of PEC boundary between two unit cells rendering more field distribution out of substrate.

3.3. PCPW with Unequal Strip Width

A more general case is considered in this section. All the dimensional parameters are normalized by the dimension of isolated CPW since the impedances are not dependent on $(W + 2S)$. This can be seen in the expression of modulus k_{eo}, k_{e1}, k_{o0}, and k_{o1} in (5), (13), (20), and (24), respectively. Figures 8 and 9 show the even- and odd-mode characteristic impedance of PCPW on top of GaAs ($\varepsilon_{rb1} = 12.9$). For a given W_g, the increase in W increases the p.u.l. capacitance and therefore reduces both the even- and odd-mode characteristic

impedance. For a given W, the increase in W_g increases the unit cell marginally. This increases the coupling surface of the conductor in the case of even mode and thus increases the p.u.l. capacitance resulting in the reduction of line impedance, while in the case of odd mode, the line impedance is slightly increased because the distance of coupling to the PEC boundary of a unit cell are also increased, reducing p.u.l. capacitance. For a large W_g, e.g., $W_g/(W + 2S) = 3$, the even-mode impedances coincide with the odd-mode ones and can be considered as the characteristic impedance of an isolated CPW with infinite lateral ground.
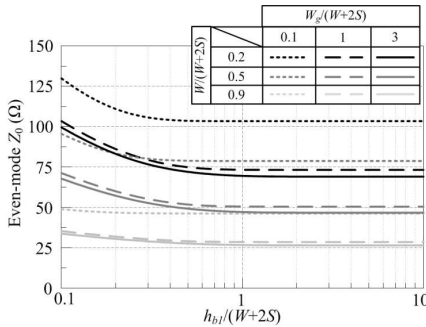

Figure 8. Even-mode characteristic impedance of PCPW on top of GaAs versus $h_{b1}/(2S + W)$.
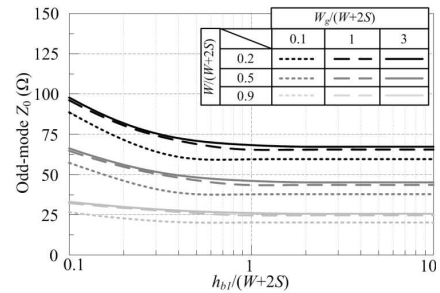
Figure 9. Odd-mode characteristic impedance of PCPW on top of GaAs versus $h_{b1}/(2S + W)$.

For a given W and W_g, the reduction of h_{b1} decreases the effective dielectric constants of the structure hence increases both the even- and odd-mode characteristic impedance of PCPW. It is worth to notice that both even- and odd-mode characteristic impedance reach saturation values for a thick substrate, where the field distribution can be considered as well-confined inside the substrate and not experienced the dielectric boundary. The saturated substrate thickness h_{b1} for characteristic impedance is dependent on each parameter, but as a rule of thumb, the PCPW can be assumed on top of infinite layer when the normalized substrate height of $h_{b1}/(2S + W)$ is larger than 1.

Figure 10 shows the even-mode characteristic impedance of PCPW on top of GaAs at $W/(W + 2S) = 0.5$ as a function of h_{b1} and W_g. As seen in Figure 10, when the width of ground is large enough, the impedance becomes constant and week coupling makes the even-mode impedance close to the odd-mode ones. As a rule of thumb, when $h_{b1} > (2S + W)$, the impedance becomes constant no matter how thick is the substrate.
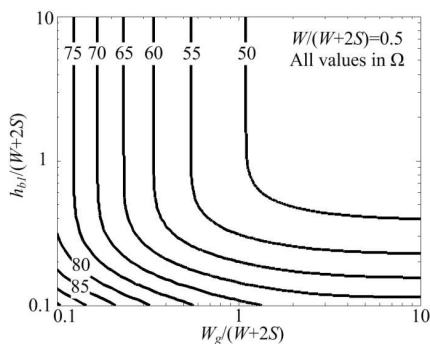
Figure 10. Design curves for the even-mode characteristic impedance as a function of W_g and h_{b1} for a PCPW with metallization ratio of 0.5 on top of GaAs.

4. CONCLUSIONS

A closed-form analytical solution has been given for obtaining the quasi-TEM properties of infinitely parallel CPWs. The presence of other CPWs at both sides of one CPW induces the coupling and alters the transmission line properties. The two contrasting cases of even- and odd-mode are discussed in this paper. The calculated results generated by the proposed formulas are in excellent agreement with those results obtained by full-wave analysis and experimental data. Using this model, it would be possible for designers to find optimum line impedance with guarding ground effects and to reduce crosstalk in coupled multiple CPW transmission lines.

REFERENCES

1. Wen, C. P., "Coplanar waveguide: A surface strip transmission line suitable for nonreciprocal gyromagnetic device applications," *IEEE Trans. on Microw. Theory and Tech.*, Vol. 17, No. 12, 1087–1090, 1969.

2. Davis, M. E., E. W. Williams, and A. C. Celestini, "Finite-boundary corrections to the coplanar waveguide analysis (short papers)," *IEEE Trans. on Microw. Theory and Tech.*, Vol. 21, No. 9, 594–596, 1973.

3. Veyres, C. and V. Fouad Hanna, "Extension of the application of conformal mapping techniques to coplanar lines with finite dimensions," *Int. J. Electron.*, Vol. 48, No. 1, 47, 1980.

4. Jackson, R. W., "Considerations in the use of coplanar waveguide for millimeter-wave integrated circuits," *IEEE Trans. on Microw. Theory and Tech.*, Vol. 34, No. 12, 1450–1456, 1986.

5. Ghione, G. and C. U. Naldi, "Coplanar waveguides for MMIC applications: Effect of upper shielding, conductor backing, finite-extent ground planes, and line-to-line coupling," *IEEE Trans. on Microw. Theory and Tech.*, Vol. 35, No. 3, 260–267, 1987.

6. Khan, O. D., A. Z. Elsherbeni, C. E. Smith, and D. Kajfez, "Characteristics of cylindrical multiconductor transmission lines above a perfectly conducting ground plane," *Progress In Electromagnetics Research*, Vol. 15, 191–220, 1997.

7. Zemanian, A. H., "A finite-difference procedure for the exterior problem inherent in capacitance computations for VLSI interconnections," *IEEE Trans. on Electron Devices*, Vol. 35, No. 7, 985–992, 1988.

8. Zemanian, A. H., R. P. Tewarson, C. P. Ju, and J. F. Jen, "Three-dimensional capacitance computations for VLSI/ULSI interconnections," *IEEE Trans. on Computer-aided Design Integrated Circuits Systems*, Vol. 8, No. 12, 1319–1326, 1989.

9. Schwindt, R. and C. Nguyen, "Spectral domain analysis of three symmetric coupled lines and application to a new bandpass filter," *IEEE Trans. on Microw. Theory and Tech.*, Vol. 42, No. 7, 1183–1189, 1994.

10. Drake, E., F. Medina, and M. Horno, "Quick computation of $[C]$ and $[L]$ matrices of generalized multiconductor coplanar waveguide transmission lines," *IEEE Trans. on Microw. Theory and Tech.*, Vol. 42, No. 12, 2328–2335, 1994.

11. Plaza, G., F. Mesa, and M. Horno, "Quick computation of $[C]$, $[L]$, $[G]$, and $[R]$ matrices of multiconductor and multilayered transmission systems," *IEEE Trans. on Microw. Theory and Tech.*, Vol. 43, No. 7, 1623–1626, 1995.

12. Yamamoto, S., T. Azakami, and K. Itakura, "Coupled strip transmission line with three center conductors," *IEEE Trans. on Microw. Theory and Tech.*, Vol. 14, No. 10, 446–461, 1966.

13. Peter Linner, L. J., "A method for the computation of the characteristic immittance matrix of multiconductor striplines with arbitrary widths," *IEEE Trans. on Microw. Theory and Tech.*, Vol. 22, No. 11, 930–937, 1974.

14. Wen, C. P., "Coplanar-waveguide directional couplers," *IEEE Trans. on Microw. Theory and Tech.*, Vol. 18, No. 6, 318–322, 1970.

15. Cheng, K. K. M., "Analysis and synthesis of coplanar coupled lines on substrates of finite thicknesses," *IEEE Trans. on Microw. Theory and Tech.*, Vol. 44, No. 4, 636–639, 1996.

16. Cheng, K. K. M., "Characteristic parameters of symmetrical triple coupled CPW lines," *Electron. Lett.*, Vol. 33, No. 8, 685–687, 1997.

17. Wolff, I., *Coplanar Microwave Integrated Circuits*, Wiley-Interscience, Hoboken, NJ, 2006.

18. Shiue, G.-H., J.-H. Shiu, and P.-W. Chiu, "Analysis and design of crosstalk noise reduction for coupled striplines inserted guard trace with an open-stub on time-domain in high-speed digital circuits," *IEEE Trans. on Comp., Packag. Manuf. Technol.*, Vol. 1, No. 10, 1573–1582, 2011.

19. Cheng, Y.-S., W.-D. Guo, C.-P. Hung, R.-B. Wu, and D. de Zutter, "Enhanced microstrip guard trace for ringing noise suppression using a dielectric superstrate," *IEEE Trans. on Adv. Packag.*, Vol. 33, No. 4, 961–968, 2010.

20. Martín, F., F. Falcone, J. Bonache, T. Lopetegi, M. A. G. Laso, and M. Sorolla, "Analysis of the reflection properties in electromagnetic bandgap coplanar waveguides loaded with reactive elements," *Progress In Electromagnetics Research*, Vol. 42, 27–48, 2003.

21. Collin, R. E., *Foundations for Microwave Engineering*, 2nd Edition, Wiley-IEEE Press, New York, 2000.

22. Erli, C. and S. Y. Chou, "Characteristics of coplanar transmission lines on multilayer substrates: Modeling and experiments," *IEEE Trans. on Microw. Theory and Tech.*, Vol. 45, No. 6, 939–945, 1997.

23. Carlsson, E. and S. Gevorgian, "Conformal mapping of the field and charge distributions in multilayered substrate CPWs," *IEEE Trans. on Microw. Theory and Tech.*, Vol. 47, No. 8, 1544–1552, 1999.

24. Ghione, G. and M. Goano, "Revisiting the partial-capacitance approach to the analysis of coplanar transmission lines on multilayered substrates," *IEEE Trans. on Microw. Theory and Tech.*, Vol. 51, No. 9, 2007–2014, 2003.

25. Chang, C.-N., Y.-C. Wong, and C. H. Chen, "Full-wave analysis of coplanar waveguides by variational conformal mapping technique," *IEEE Trans. on Microw. Theory and Tech.*, Vol. 38, No. 9, 1339–1344, 1990.

26. Jansen, R. H., "Hybrid mode analysis of end effects of planar microwave and millimetrewave transmission lines," *IEE Proc. H Microw. Optics and Antennas*, Vol. 128, No. 2, 77–86, 1981.

27. *COMSOL Multiphysics*, v4.2a Ed., 2011.